ELSEVIER

Journal of Photochemistry and Photobiology A: Chemistry 105 (1997) 1–6

Journal of PHOTOCHEMISTRY AND PHOTOBIOLOGY A:CHEMISTRY

High-temperature UV–visible absorption spectral measurements and estimated primary photodissociation rates of formaldehyde, chlorobenzene and 1-chloronaphthalene

Michael W. Mackey [a], John W. Daily [a,*], J. Thomas McKinnon [b], Edward P. Riedel [a]

[a] *Center for Combustion Research, Department of Mechanical Engineering, University of Colorado at Boulder, Boulder, CO 80309-0427, USA*

[b] *Chemical Engineering Department, Colorado School of Mines, Golden, CO, USA*

Received 1 June 1995; revised 13 September 1996; accepted 7 October 1996

Abstract

Measurements of the high-temperature UV–visible absorption spectra of formaldehyde, chlorobenzene and 1-chloronaphthalene and estimates of their high-temperature photodissociation rates are presented. The photodissociation rate estimates were based on the measured absorption spectra and an assumed direct terrestrial spectral radiant flux for a 1.5 air mass atmosphere. The results indicate a strong dependence of the solar photodissociation rate on the temperature. © 1997 Elsevier Science S.A.

Keywords: Chlorobenzene; 1-Chloronaphthalene; Formaldehyde; High temperature; Primary photodissociation rate; UV–visible absorption

1. Introduction

In a study [1] carried out for the National Renewable Energy Laboratory (NREL), calculations indicated that concentrated solar radiation may enhance certain thermal hazardous waste destruction processes. Enhancement is achieved when chemical species in the destruction process absorb solar photons and photodissociate into radical species. These radical species may initiate chain branching reactions, resulting in a net enhancement of the hazardous waste destruction processes.

The photodissociation rates of the various species are the key to the evaluation of the degree of enhancement achieved using concentrated sunlight. The accuracy of the NREL model was limited because the photodissociation rates were based on room-temperature absorption and quantum yield data. The solar-induced photodissociation rates at the typical operating temperatures (400–800 °C) for hazardous destruction processes may differ significantly from the room-temperature rates due to an expected red shift in the absorption spectra and an associated increase in the integrated solar absorptivity.

To improve the accuracy of the NREL model, the high-temperature absorption spectra of formaldehyde (CH_2O), chlorobenzene ($1\text{-}C_6H_5Cl$) and 1-chloronaphthalene ($1\text{-}C_{10}H_7Cl$) were measured. Based on the spectral absorption measurements, the high-temperature photodissociation rates were estimated. In this paper, the system developed to measure the absorption at high temperatures and the procedure used to estimate the primary photodissociation rates are presented. The results of the measurements are then given and discussed.

2. Experimental details

2.1. High-temperature molar absorptivity measurements

Molar absorptivity measurements were made at 0.8 atm in a temperature-controlled, flow-tube absorption cell, with evacuated double pane quartz windows. The system is illustrated in Fig. 1. Nitrogen was used as the diluent carrier gas for each absorbing species. The absorption cell was illuminated with a single light beam generated by an Oriel 75 W xenon arc lamp. The lamp intensity was significantly attenuated before reaching the cell, thus reducing the possibility of photochemical reactions. The light beam was dispersed with a Jarrell-Ash model 82-499 spectrograph. The spectral intensity of the attenuated lamp beam was monitored in the 250–450 nm wavelength region with a Princeton Instruments model IVY-700 microchannel plate intensified photodiode array detector. The slit/grating combination was such that the spectral resolution was 0.3 nm.

* Corresponding author. Tel.: +1 303 492 7110; fax: +1 303 492 2863; e-mail: daily@spot.colorado.edu

PII S1010-6030(97)00066-X

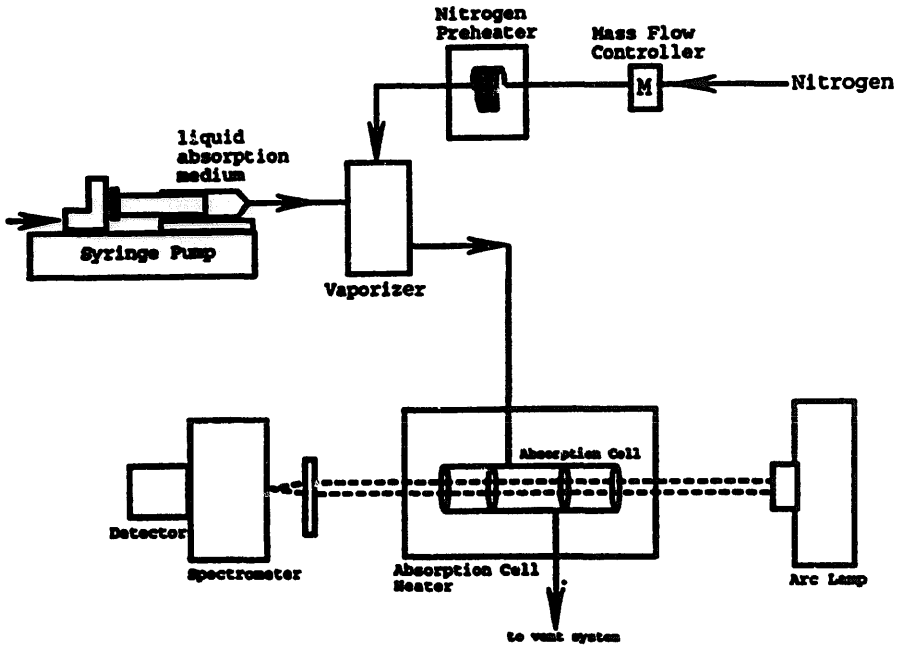

Fig. 1. Schematic diagram of system for high-temperature spectral measurements.

The liquid samples (99.9% reagent grade) were injected at a constant rate into a vaporizer and diluted with nitrogen gas as shown in Fig. 1. A steady vaporization rate was obtained by injecting the liquid directly onto the hot surface of the vaporizer which was held 20–30 °C above the boiling point. The vapor and nitrogen gas were mixed and preheated to the desired temperature prior to flowing into the absorption cell. The temperature inside the absorption cell was maintained by a temperature-controlled tube furnace.

The molar absorptivity was determined by applying the Beer–Lambert law ($\log_{10}$ definition) to the measured transmissivity spectrum at a single absorbing species concentration. The ideal gas mixture assumption was used to determine the concentration together with the measured values of the mass flow rates, pressure and temperature.

The linear relationship between the absorbing species concentration and the absorbance stated by the Beer–Lambert law was verified by measuring the absorptivity at several different concentrations. Changes in concentration were made by changing the liquid injection rate and/or the nitrogen gas flow rate. The results show excellent agreement between the molar absorptivity measurements made at different concentrations.

2.2. *Uncertainty analysis*

An uncertainty analysis was carried out to explore the propagation of the random uncertainty into the calculated molar absorptivity. The propagation relation takes the form [2]

$$\omega_R = \left\{ \left[\frac{\partial R}{\partial \nu_1} \omega_1 \right]^2 + \left[\frac{\partial R}{\partial \nu_2} \omega_2 \right]^2 + \cdots + \left[\frac{\partial R}{\partial \nu_i} \omega_i \right]^2 \right\}^{1/2}$$

where ω_R represents the uncertainty in the calculated result R and ω_i represents the uncertainty in each value ν_i used to calculate the result. Applying this equation to the Beer–Lambert law yields the following equation

$$\frac{\omega_\epsilon(\lambda)}{\epsilon(\lambda)} = \left\{ \left[\frac{1}{\ln[T(\lambda)]} \frac{\omega_T(\lambda)}{T(\lambda)} \right]^2 + \left[\frac{\omega_b}{b} \right]^2 + \left[\frac{\omega_c}{c} \right]^2 \right\}^{1/2}$$

where $\epsilon(\lambda)$, $T(\lambda)$, b and c represent the molar absorptivity, transmissivity, optical path length and species concentration respectively and $\omega_\epsilon(\lambda)$, $\omega_T(\lambda)$, ω_b and ω_c represent the uncertainties in these variables. Typical values and uncertainties are given in Table 1.

To minimize the random errors in the absorptivity measurements, all absorptivity data presented are the average of 20–40 individual absorptivity spectra at a given temperature. The error bars presented in Tables 2–4 represent ± 2 standard deviations in the calculated absorptivity due to this averaging process. The agreement between individual spectral measurements is within 1% of the calculated average.

2.3. *Estimation of the photodissociation reaction rates*

Based on the measured molar absorptivity at each temperature, the primary photodissociation rates can be determined from the following equation

Table 1
Typical values and uncertainties of experimental variables

Name	Symbol	Value	Uncertainty (95% confidence)
Molar absorptivity	$\epsilon(\lambda)$	Varies	Function of temperature
Transmissivity	$T(\lambda)$	10–100%	Function of temperature
Optical path length	b	10.05 cm	0.6%
Species concentration	c	Varies	<2%

Table 2
Formaldehyde 10 nm bandwidth average absorption spectra at different temperatures

Wavelength (nm)	Log_{10} molar absorptivity (cm^{-1} l mol^{-1})					
	150 °C	250 °C	300 °C	400 °C	500 °C	600 °C
270–279	3.42±0.07	3.9±0.1	3.5±0.1	4.5±0.2	5.7±0.1	5.7±0.1
280–289	4.71±0.07	5.2±0.1	4.9±0.1	5.2±0.2	7.4±0.1	7.1±0.1
290–299	6.03±0.08	6.4±0.1	6.3±0.1	6.7±0.2	8.8±0.1	8.6±0.1
300–309	6.78±0.08	7.1±0.1	7.0±0.1	7.4±0.2	9.5±0.1	9.4±0.1
310–319	6.44±0.08	6.8±0.1	6.8±0.1	7.3±0.2	9.2±0.1	9.3±0.1
320–329	5.39±0.08	5.7±0.1	5.8±0.1	6.3±0.2	7.8±0.1	8.1±0.1
330–339	3.23±0.07	3.5±0.1	3.7±0.1	3.9±0.2	5.1±0.1	5.7±0.1
340–349	1.74±0.07	2.1±0.1	2.3±0.1	2.1±0.2	3.5±0.1	4.1±0.1
350–359	1.51±0.06	1.9±0.1	1.9±0.1	2.0±0.2	3.1±0.1	3.5±0.1
360–369	0.35±0.06	0.4±0.1	0.4±0.1	0.4±0.2	0.94±0.08	1.27±0.07
370–379	0.26±0.06	0.3±0.1	[a]	[a]	0.78±0.08	0.98±0.07
380–389	[a]	[a]	[a]	[a]	0.31±0.08	0.38±0.07
390–399	[a]	[a]	[a]	[a]	[a]	0.17±0.07

[a]Estimated uncertainty was greater than the measured absorptivity.

Table 3
Chlorobenzene 10 nm bandwidth average absorption spectra

Wavelength (nm)	Log_{10} molar absorptivity (cm^{-1} l mol^{-1})					
	200 °C	300 °C	400 °C	500 °C	600 °C	700 °C
260	128±1	137±1	162±1	167±2	181±5	188±3
270	60±0.5	70±0.5	100±0.7	118±1	148±4	168±3
280	5±0.2	9.8±0.2	26.5±0.3	36.1±0.5	65±2	89±2
290	[a]	[a]	7.4±0.2	8.0±0.4	18.6±0.8	29.7±0.7
300	[a]	[a]	[a]	1.3±0.7	5.6±0.7	7.6±0.5
310	[a]	[a]	[a]	[a]	2.0±0.7	2.3±0.4

[a]Estimated uncertainty was greater than the measured absorptivity.

Table 4
1-Chloronaphthalene 10 nm bandwidth average absorption spectra

Wavelength (nm)	Log_{10} molar absorptivity (cm^{-1} l mol^{-1})				
	300 °C	400 °C	500 °C	600 °C	700 °C
260	4140±40	4020±70	4330±40	4300±100	4070±70
270	4710±40	4780±70	4920±40	4900±100	4940±70
280	3610±30	3900±60	4090±30	4310±90	4510±60
290	1330±10	1710±30	2070±20	2520±50	2820±40
300	404±6	550±10	763±7	1100±30	1300±20
310	210±5	273±9	370±6	610±30	640±20
320	76±5	117±8	182±5	180±20	350±10
330	11±5	23±7	61±5	61±20	170±10
340	[a]	[a]	13±8	150±20	70±10

[a]Estimated uncertainty was greater than the measured absorptivity.

$$k = \int_{\lambda=0}^{\lambda=\infty} \epsilon(\lambda)_e \cdot QY(\lambda) \cdot \Phi_0(\lambda) \cdot d\lambda$$

where k is the photodissociation rate (s^{-1}), λ is the light wavelength (nm), $\epsilon(\lambda)_e$ is the measured molar absorptivity (log_e) ($l\,mol^{-1}\,cm^{-1}$), $QY(\lambda)$ is the primary quantum yield (photon^{-1}) and $\Phi_0(\lambda)$ is the incident radiant flux (photon $cm^{-2}\,s^{-1}\,nm^{-1}$).

For this work, results for the molar absorptivity were calculated using the log_{10} definition of the Beer–Lambert law. Conversion of the results presented in the log_{10} form to log_e can be performed using the following relation

$$\epsilon(\lambda)_e = 2.3026\epsilon(\lambda)_{10}$$

A 1.5 air mass direct terrestrial spectral radiant flux given by Hulstrom et al. [3] was assumed for the incident radiation. The solar cut-off for the data of Hulstrom et al. is approximately 305 nm. This differs from the accepted cut-off for actinic solar flux of approximately 290 nm. This discrepancy is due to the fact that actinic solar flux is composed of direct

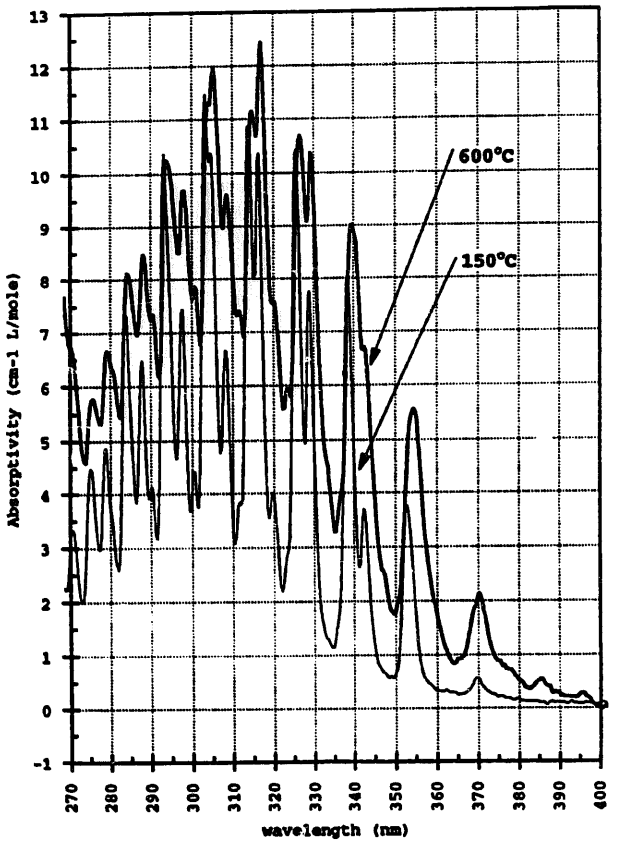

Fig. 2. Formaldehyde absorption spectra.

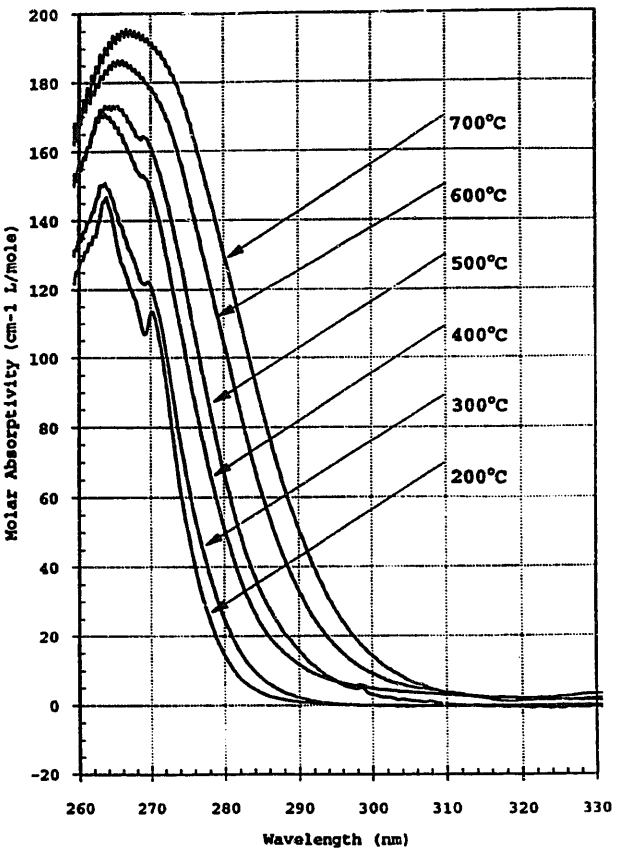

Fig. 3. Chlorobenzene absorption spectra.

and diffuse radiation [4], and this research was performed in order to model a solar process in which the sun's radiant flux would probably be focused thus eliminating the use of diffuse radiation. Therefore only the sun's direct radiant flux as given by Hulstrom et al. was used for the rate calculations. A formaldehyde room-temperature primary quantum yield spectrum given by Finlayson-Pitts and Pitts [4] was used to evaluate the formaldehyde photodissociation rates at temperatures of 150–600 °C. Because no primary quantum yield data at any temperature were available for chlorobenzene and 1-chloronaphthalene, a primary quantum yield of unity (one molecule dissociated per photon absorbed) was assumed for all temperatures and wavelengths.

3. Results

Molar absorptivity spectral measurements of formaldehyde, chlorobenzene and 1-chloronaphthalene are given in Figs. 2–4 respectively. To illustrate the temperature dependence of the measured molar absorptivity, a 10 nm bandwidth average molar absorptivity spectrum for each species is given in Figs. 5–7 and is summarized in Tables 1–3. This 10 nm bandwidth average format clearly shows the changes in molar absorptivity with increasing temperature. Increases in the absorption spectra at wavelengths greater than 305 nm (the solar spectrum cut-off for direct terrestrial solar flux) result in an increase in the estimated photodissociation rate for terrestrial solar absorption. Any changes in the absorption spectrum below 305 nm do not affect the estimated photodissociation rate because 305 nm is the low-wavelength cut-off of the direct terrestrial solar spectrum [3].

Based on the absorptivity measurements, the photodissociation rates were estimated at each temperature. The results were then plotted in Arrhenius form, where the natural logarithm of the calculated rate at a certain temperature is plotted against the inverse of the product of R_g (ideal gas constant) and temperature. The data plotted in this manner usually result in a straight line. Therefore a regression analysis was performed to fit the temperature dependence of the photodissociation rate to the following equation

$$\ln k = A - E_a(1/R_gT)$$

where A (the Arrhenius factor) represents the intercept of the regression line fit at the $\ln k$ axis and E_a (the activation energy) represents the slope of the regression line fit. The regression results are given in Table 5 and plotted in Figs. 8–11.

Provided that the quantum yield assumptions used for the photolysis rate calculations are valid, the results indicate a very strong dependence of the photodissociation rate on the temperature. There is the possibility that the quantum yields for the compounds discussed are much different than the assumed values. Therefore, in the absence of high-temperature quantum yield data for these compounds, the rates presented in this paper are merely estimations.

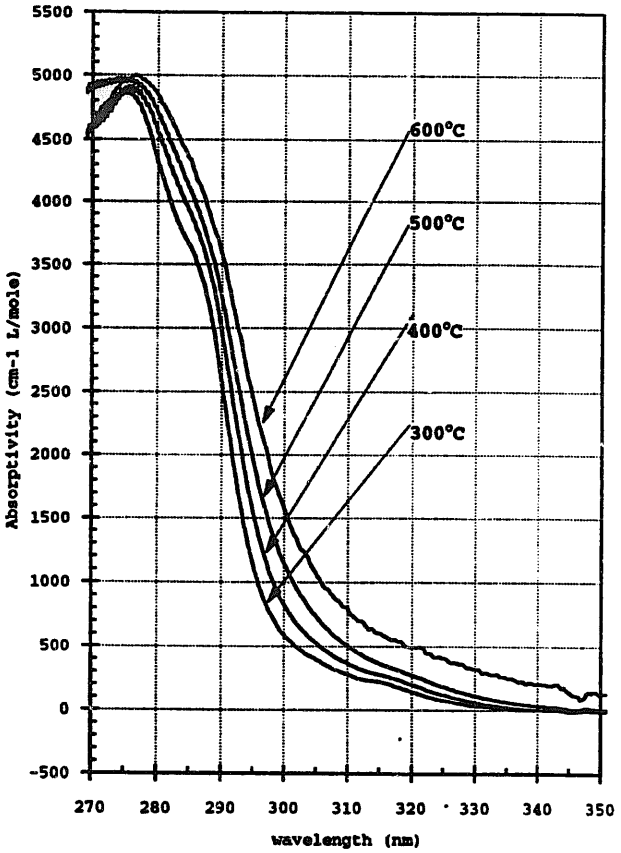

Fig. 4. 1-Chloronaphthalene absorption spectra.

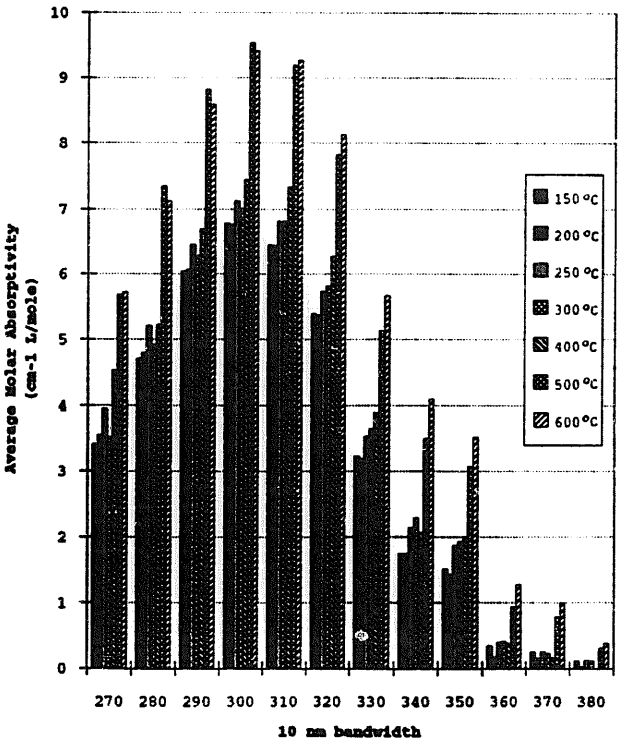

Fig. 5. Formaldehyde 10 nm bandwidth average absorption spectra.

4. Conclusions

A system has been established to measure the molar absorptivity at temperatures up to 700 °C with excellent

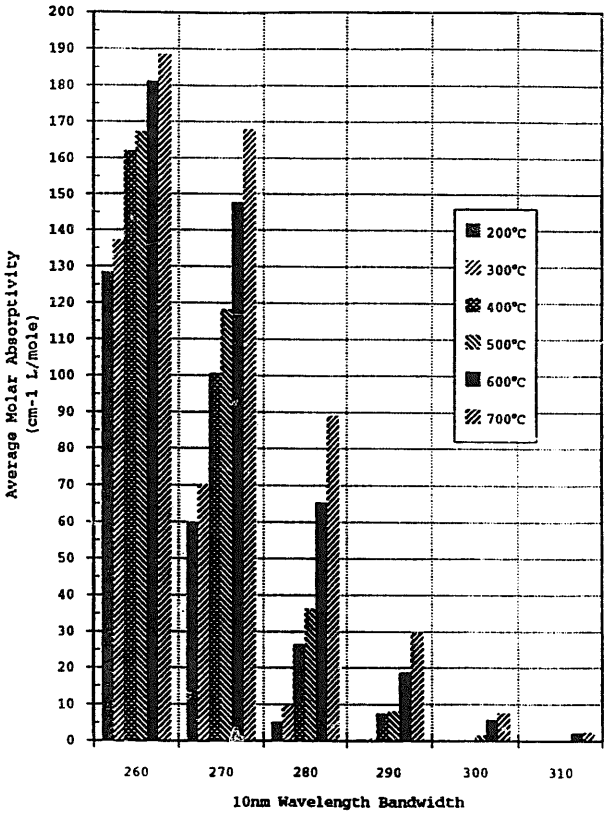

Fig. 6. Chlorobenzene 10 nm bandwidth average absorption spectra.

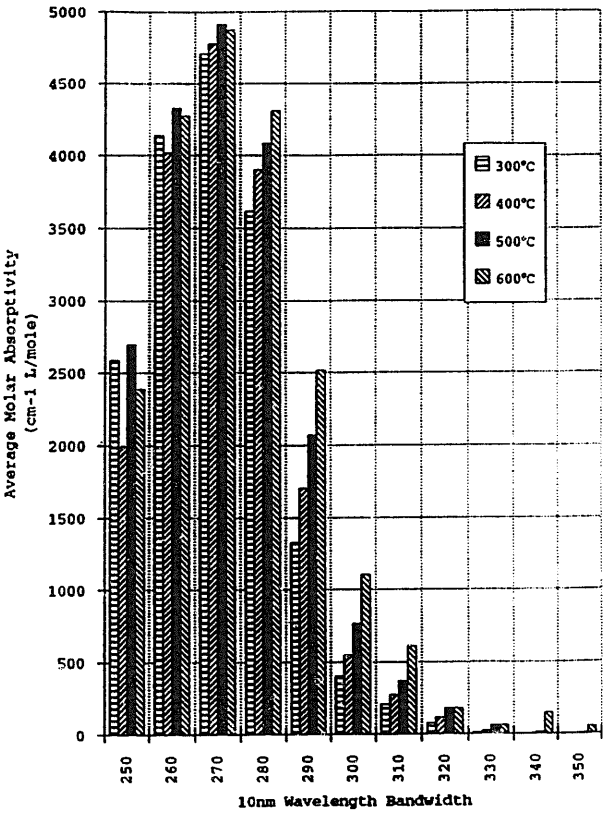

Fig. 7. 1-Chloronaphthalene 10 nm bandwidth average absorption spectra.

Table 5
Estimated photodissociation reaction rates ($A \exp(-E_a/R_gT)$) for terrestrial solar spectrum absorption

Photodissociation reaction	Temperature range (°C)	A (s^{-1})	E_a (J mol^{-1})
$CH_2O + h\nu \rightarrow HCO + H$	150–600	3.5×10^{-5}	742
$CH_2O + h\nu \rightarrow CO + H_2$	150–600	4.6×10^{-5}	997
$C_6H_5Cl + h\nu \rightarrow C_6H_5 + Cl$	500–700	0.062	16300
$C_{10}H_7Cl + h\nu \rightarrow C_{10}H_7 + Cl$	300–600	0.024	3970

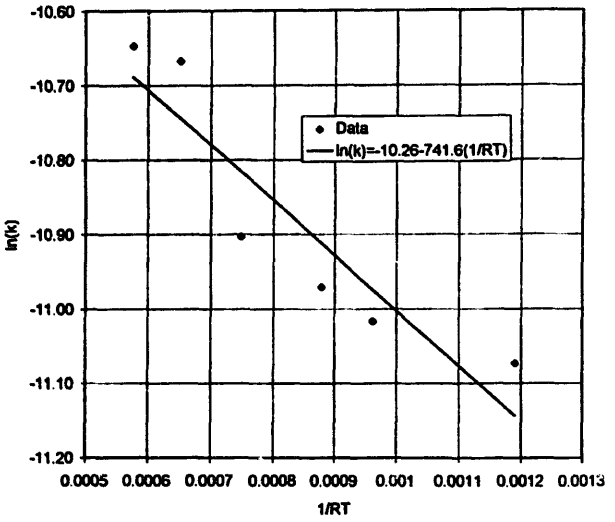

Fig. 8. Estimated rate of formaldehyde photodissociation into formyl and hydrogen as a function of temperature, using room-temperature quantum yield data.

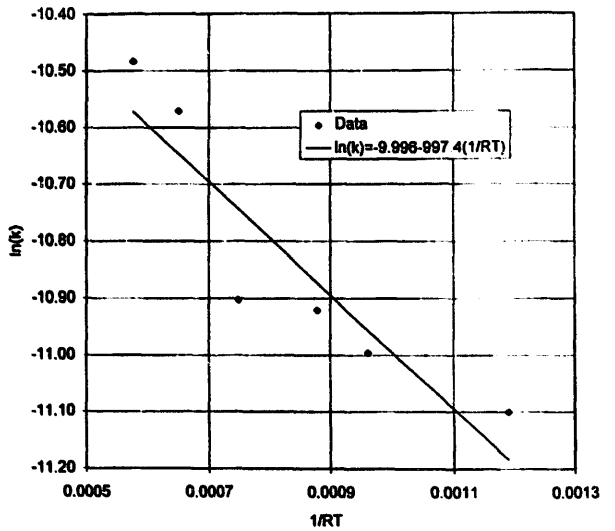

Fig. 9. Estimated rate of formaldehyde photodissociation into diatomic hydrogen and carbon monoxide as a function of temperature, using room-temperature quantum yield data.

repeatability, and measurements were made for formaldehyde, chlorobenzene and 1-chloronaphthalene. Based on the molar absorptivity measurements, the primary photodissociation rates were estimated for incident radiation equivalent to a 1.5 air mass direct terrestrial solar spectrum. The results illustrate the strong temperature dependence of the solar absorptivity and photodissociation rate (for assumed quantum yield data).

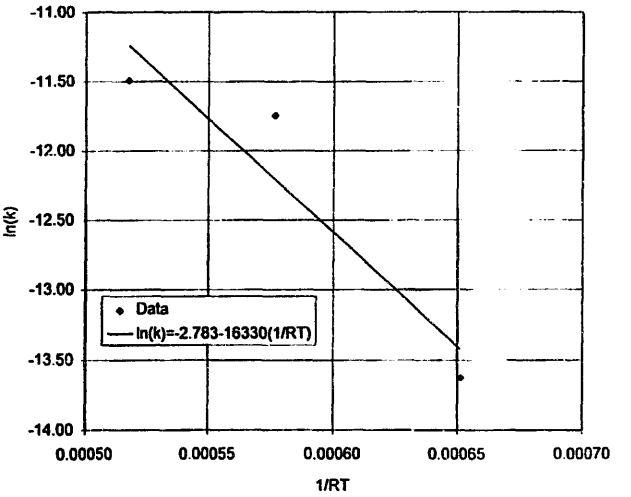

Fig. 10. Estimated rate of chlorobenzene photodissociation into phenyl and chlorine as a function of temperature assuming a quantum yield equal to unity.

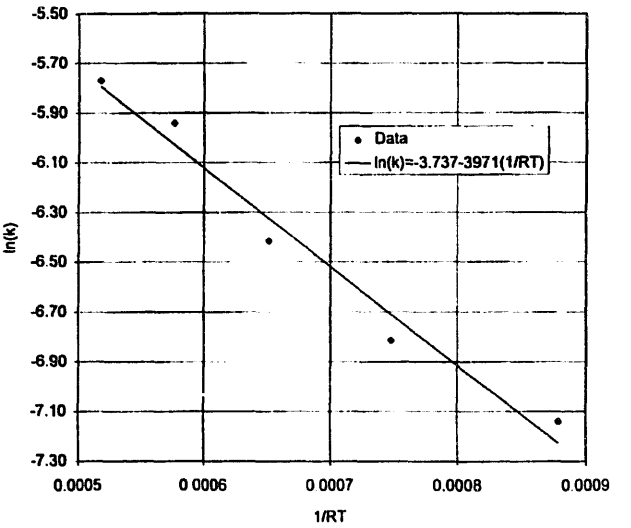

Fig. 11. Estimated rate of 1-chloronaphthalene photodissociation into naphthalenyl and chlorine as a function of temperature assuming a quantum yield equal to unity.

References

[1] M.R. Nimlos, T.A. Milne, J.T. McKinnon, Photothermal oxidative destruction of 1-chloronaphthalene, Environ. Sci. Technol. 28 (1994) 816–822.
[2] J.R. Taylor, An Introduction to Error Analysis, University Science Books, Mill Valley, CA, 1982.
[3] R. Hulstrom, R. Bird, C. Riordan, Solar Cells 15 (1985) 365–391.
[4] B.J. Finlayson-Pitts, J.N. Pitts, Atmospheric Chemistry, Wiley, New York, 1986.